

Spectroscopic Measurement of Solid Solubility in Supercritical Fluids

Truc T. Ngo, David Bush, and Charles A. Eckert

School of Chemical Engineering and Specialty Separations Center, Georgia Institute of Technology,
Atlanta, GA 30332

Charles L. Liotta

School of Chemistry and Biochemistry & Specialty Separations Center, Georgia Institute of Technology,
Atlanta, GA 30332

Different in situ spectroscopic techniques, including infrared, ultraviolet, and fluorescence, were developed to measure the solubility of organic solids in supercritical carbon dioxide (scCO₂). These techniques are applicable over a wide range of concentrations, as low as 10⁻⁶ or 10⁻⁷ mol fraction, where the conventional flow method is ineffective and less accurate. No separate calibration is required; in fact, the molar absorptivity is determined at the saturation point as an additional benefit. While this technique requires more time per data point, it is more accurate and unbiased than traditional methods at lower concentrations. The Patel-Teja equation of state was used to correlate the data and expand the data for the ternary system. Data are reported for anthracene, 1,4-naphthoquinone, and 2-naphthol in scCO₂ and CO₂ with methanol cosolvent at 313 K and a pressure range from 7 to 21 MPa.

Introduction

Because supercritical fluids, particularly supercritical CO₂ (scCO₂), have a wide range of applications in various chemical processes, it is necessary to know accurately the solubility of different organic solutes in the fluid. The most common method for obtaining solubility data is the dynamic flow (or transpiration) technique. This method often encountered some experimental difficulties in valve clogging and sampling of saturated mixture, which could result in inaccurate data measurements (McHugh and Krukonis, 1994). We have compiled a database for the solubility of approximately 300 compounds in scCO₂. If we compare data measured by different laboratories, where the solubility is relatively high (that is, naphthalene), there is good agreement. However, when the solubility is 10⁻⁴ mol fraction or lower (that is, anthracene or octacosane), there is much less agreement. Figure 1 illustrates this point.

In situ spectroscopy is another powerful tool to measure solubility. It requires no sampling, which overcomes many of the deficiencies of the flow method. Various types of work

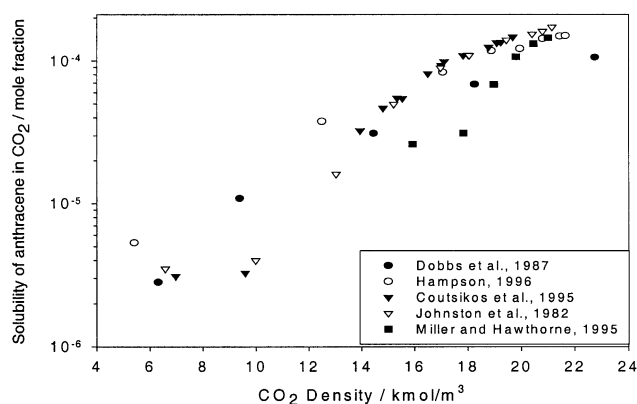


Figure 1. Inconsistency in flow method at low concentration regions; data reported at 323 K.

have been reported in the literature for the past twenty years, either using FT-IR or UV/Visible spectroscopy (Ebeling and Franck, 1984; Zerda et al., 1986; Cygnarowicz et al., 1990;

Correspondence concerning this article should be addressed to C. A. Eckert.

Jackson et al., 1995; West et al., 1998). However, spectroscopy has been applied incorrectly by assuming these false assumptions: the molar absorptivity (ϵ) of a solute in CO₂ is the same as in liquid solvents (Ebeling and Franck, 1984; Cygnarowicz et al., 1990), the molar absorptivity does not change with CO₂ density (Ebeling and Franck, 1984; Zerda et al., 1986; Cygnarowicz et al., 1990), the wavelength of peak maximum (λ_{max}) does not change with CO₂ density (Ebeling and Franck, 1984; Cygnarowicz et al., 1990). Rice et al. (1995) have shown that ϵ can increase up to almost threefold when CO₂ density goes from 300 kg/m³ to 900 kg/m³. Moreover, change in fluid density can also result in a significant spectral shift (Inomata et al., 1993; Rice et al., 1995), as much as 5 nm in wavelength based on our experiments with 1,4-naphthoquinone. According to Rice et al. (1995), ϵ increases by a factor of 2.7 for pyrene and 2.2 for anthracene as a result of analyzing peak absorbances at a fixed wavelength. As a consequence, neglecting these changes can yield an error up to 500% in solubility (Rice et al., 1995).

In this article, we show how different spectroscopic techniques, including infrared (IR), ultraviolet (UV), and fluorescence, can be used to measure the solubility of different organic compounds in supercritical carbon dioxide. We are able to obtain solubility data over a wide range of concentrations, as low as 10⁻⁷ mol fraction, without performing any calibration prior to the experiments or making any assumptions on the constancy of the molar absorptivity. We also show the effect of cosolvent on the solubility behavior of different organic compounds having different functional groups. This behavior was studied by using the UV spectroscopic technique.

Experimental Apparatus and Procedure

Apparatus

As mentioned earlier, three different spectroscopic techniques, including IR, UV/Vis, and fluorescence, were demonstrated using the Bruker Vector 22 IR spectrophotometer, the HP 8453 UV/Vis spectrophotometer, and the Shimadzu RF-5301PC Spectrofluorophotometer, respectively. All the experiments were carried out in high-pressure optical cells (Kazarian et al., 1996), having two parallel paths with either quartz or barium fluoride (BaF₂) windows. Since quartz does not absorb in UV or visible ranges, it is suitable for UV/Vis and fluorescence experiments. However, quartz shows strong absorption in the IR region, and therefore BaF₂ was used in IR experiments.

The path lengths can be varied from 0.003 m to 0.054 m to suit a range of measured concentrations. For the fluorescence experiments, another window was added to one end of the cell to allow the 90° angle of emission signals. The solution mixture was constantly stirred during the experiment by two stir bars placed at the bottom of the cell, to promote the diffusion of solute into the fluid phase, and to keep the conditions uniform inside the cell. The temperature was measured by an Omega Type-K thermocouple in contact with the fluid; pressure was read from a Druck pressure gauge connected to the cell through a short line of tubing, accurate to ± 0.02 MPa. The cell temperature was controlled to within 0.5 K with six cartridge heaters. Carbon dioxide was introduced into the cell using an Isco syringe pump.

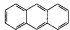
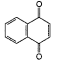
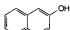
Materials

The solutes used in this experiment, with at least 99% purity, were purchased from the Aldrich Chemical Company, Inc. and Fluka Chemika. They are listed in Table 1, along with some important physical properties. A.C.S. HPLC methanol of 99.93% purity was obtained from the Aldrich Chemical Company, Inc. SFC-grade carbon dioxide, purchased from Matheson with at least 99.99% purity, was passed through a water filter before use.

Procedure

All experiments were performed at 313 K, with pressures ranging from 7 MPa to 21 MPa. Known amounts of solutes were introduced to the cell in solid form (>0.01 g) or in solution (<0.01 g). When the solute was added in solution form, the cell was heated up to 313 K to allow the solvent to evaporate. We started out with the smallest possible amount of solid, based on the chemical structure of the organic compound, and increased to the maximum limit. After loading, the cell was placed under vacuum (approximately 100 Pa) for one hour. A negligible amount of the solute is believed to have escaped. To prove this, for 1,4-naphthoquinone (which has the highest vapor pressure among the three compounds), the solid in the cell after vacuum was redissolved in methanol to determine the amount that had escaped during the vacuum process. The result shows that the loss was not detectable by UV.

Table 1. Physical Properties of Solutes

Compound	Structure	T_m (K)	P^{sub} (Pa)	T_c (K)	P_c (MPa)	ζ_c	F
Anthracene		488–492	0.006*	873	2.9	0.2689	0.8597
1,4-Naphthoquinone		396–398	0.4**	792.2	4.12	0.28	1.0045
2-Naphthol		394–395	0.125†	811.4	4.74	0.3214	1.2462

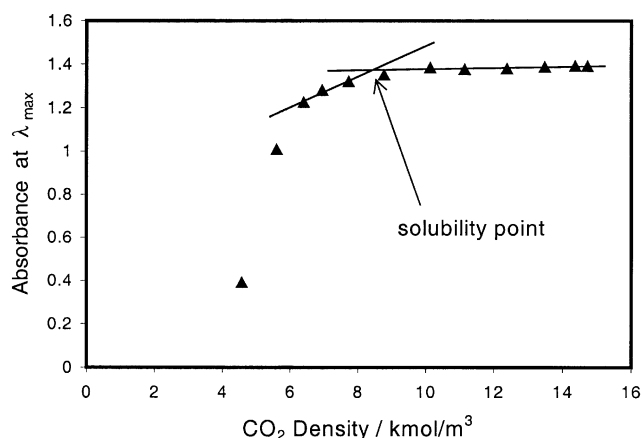
* Hansen and Eckert, 1986.

** De Kruif et al., 1981.

† Colomina et al., 1974.

Table 2. Solubility of Anthracene in Pure CO₂ at 313 K

Spectroscopic Technique	<i>P</i> (MPa)	Density (kmol/m ³)	Concentration (kmol/m ³)	Mol Fraction (mol Solute/mol CO ₂)
IR	20.88	19.3	1.73×10^{-3}	8.98×10^{-5}
	16.70	18.3	1.91×10^{-3}	6.51×10^{-5}
	14.41	17.5	9.40×10^{-4}	5.36×10^{-5}
	12.46	16.6	8.07×10^{-4}	4.86×10^{-5}
	10.69	15.2	4.07×10^{-4}	2.67×10^{-5}
UV/Vis	11.11	15.6	4.15×10^{-4}	2.65×10^{-5}
	9.20	12.0	1.05×10^{-4}	8.72×10^{-6}
	8.82	9.9	6.99×10^{-5}	7.06×10^{-6}
	8.74	9.5	6.99×10^{-5}	7.39×10^{-6}
	8.54	8.3	3.49×10^{-5}	4.20×10^{-6}
	8.26	7.1	1.40×10^{-5}	1.96×10^{-6}
Fluorescence	8.16	6.8	1.13×10^{-5}	1.66×10^{-6}
	7.53	5.3	4.60×10^{-6}	8.66×10^{-7}
	7.08	4.6	2.30×10^{-6}	4.99×10^{-7}

**Figure 2. UV absorbance of 1,4-naphthoquinone in pure CO₂ as a function of CO₂ density (solubility of 3.03×10^{-5} mol/mol).**

The cell was then pressurized with carbon dioxide, and stirred constantly. Equilibrium of the mixture was observed *in situ* by periodically taking spectra of the solution. CO₂ pressure was ramped up until there was no further significant increase in the peak absorbance. This meant that all solids had been dissolved in the fluid phase. For the experiments to study cosolvent effect, methanol was added using different sizes of sample loops and a six-port valve.

The absorbance (or emission, in the case of fluorescence) was plotted versus CO₂ density (an example is shown in Figure 2). As the density increased, there was a large increase in solubility. Once all the solute in the cell dissolved, there was an abrupt change in the slope. The absorbance still increased slightly due to the change in molar absorptivity. The density at saturation was then determined from the intersection of the two linear regions on the graph. At this point, solubility can be calculated by knowing the exact mass of solute loaded into the cell, the fluid density at saturation, and the cell volume. The density of pure CO₂ was calculated from the Jacobsen and Stewart MBWR equation of state (Ely et al., 1989). The density of the CO₂-methanol mixture was calculated from the Patel-Teja (P-T) equation of state. To get ac-

Table 3. Solubility of 1,4-Naphthoquinone in CO₂ and Methanol Cosolvent at 313 K

<i>P</i> (MPa)	Methanol Mol Fraction (mol %)	Density (kmol/m ³)	Concentration (kmol/m ³)	Mol Fraction (mol Solute/mol CO ₂)
12.30	0	16.5	2.53×10^{-2}	1.53×10^{-3}
9.76	0	13.8	1.05×10^{-2}	7.61×10^{-4}
9.52	0	13.2	7.22×10^{-3}	5.47×10^{-4}
9.00	0	11.0	2.06×10^{-3}	1.87×10^{-4}
8.83	0	10.0	1.23×10^{-3}	1.23×10^{-4}
8.53	0	8.2	2.50×10^{-4}	3.03×10^{-5}
8.46	0	7.9	1.29×10^{-4}	1.63×10^{-5}
12.22	1.79	16.9	5.05×10^{-2}	2.99×10^{-3}
10.07	1.04	14.9	2.53×10^{-2}	1.70×10^{-3}
8.90	2.37	12.8	2.53×10^{-2}	1.98×10^{-3}

curate densities, the P-T volume translation term for CO₂, which is normally determined from critical properties, was fit so that the P-T equation of state gave the same results as the MBWR equation for pure CO₂ densities. Densities of CO₂-methanol mixtures calculated this way matched Berger's data (1991) with an average error of 1.5%.

Results

Each solubility point was determined from the plot of peak absorbance versus CO₂ density. Different absorption or emission peaks were selected to determine the point at saturation for each compound. The values obtained from these

Table 4. Solubility of 2-Naphthol in CO₂ and Methanol Cosolvent at 313 K

<i>P</i> (MPa)	Methanol Mol Fraction (mol %)	Density (kmol/m ³)	Concentration (kmol/m ³)	Mol Fraction (mol Solute/mol CO ₂)
18.07	0	18.8	1.01×10^{-2}	5.39×10^{-4}
12.27	0	16.5	5.12×10^{-3}	3.10×10^{-4}
9.56	0	12.9	1.55×10^{-3}	1.20×10^{-4}
8.85	0	9.9	5.69×10^{-4}	5.74×10^{-5}
12.41	1.00	17.1	1.01×10^{-2}	5.92×10^{-4}
9.28	2.25	14.8	1.24×10^{-2}	8.38×10^{-4}
8.52	5.14	13.6	2.04×10^{-2}	1.50×10^{-3}

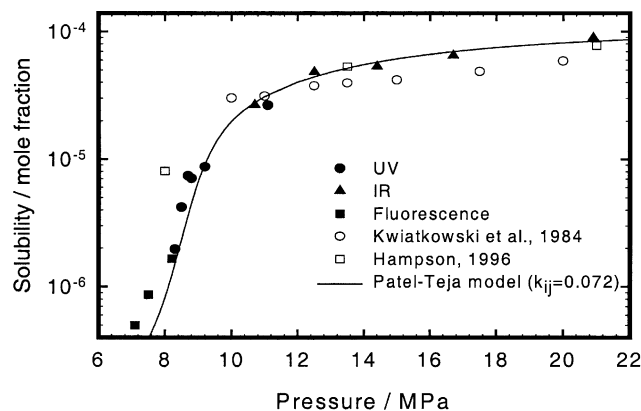


Figure 3. Solubility of anthracene in pure CO₂ at 313 K.

peaks are very consistent with one another. The results are listed in Tables 2, 3 and 4.

The solubility of anthracene was measured in pure CO₂ using all three spectroscopic techniques: IR, UV, and fluorescence. In IR, the C-H stretching vibrations at 3065 cm⁻¹ and 881 cm⁻¹ were used for data analysis; whereas, in UV, the absorption peaks in wavelength range from 315 nm to 369 nm, and in fluorescence, the emission peaks at 367 nm–425 nm were followed. Table 2 summarizes the solubility results obtained for anthracene in terms of both concentrations and mol fractions as functions of CO₂ pressure and density. The uncertainties in the measured solubility range from 1% to 5%. The graph is shown in Figure 3. Several absorption peaks were used, but as an example, for the peak maximum at 349 nm, the average molar absorptivity of anthracene at saturation was calculated to be 6.89×10^5 m²/kmol with 11% variation over the concentration range from 1.40×10^{-5} kmol/m³ to 4.15×10^{-4} kmol/m³ and the CO₂ density range from 7.1 kmol/m³ to 15.6 kmol/m³. Literature data have shown that at a fixed concentration, the molar absorptivity of anthracene can increase by as much as 30% over that same range of CO₂ density (Rice et al., 1995). However, the scatter in our data precluded observation of any trend.

The solubilities of 1,4-naphthoquinone and 2-naphthol were measured in both pure CO₂ and CO₂ with methanol cosolvent using UV spectroscopy. The UV peak at around 322 nm was used to follow the increase in concentration of 1,4-naphthoquinone in the fluid phase. The UV peaks at 261 nm, 270 nm, 282 nm, 312 nm, and 326 nm were used for 2-naphthol. The solubility results are reported in Tables 3 and 4, respectively, and graphically presented in Figures 4, 5, 6, and 7.

Discussion

UV and IR measurements were based on the principles of Lambert–Beer's law:

$$A = \epsilon l C,$$

where A is defined as the absorbance, ϵ (m²/kmol) is the molar absorptivity, l (m) is the optical path length, and C (kmol/m³) is the concentration of solute in the fluid phase.

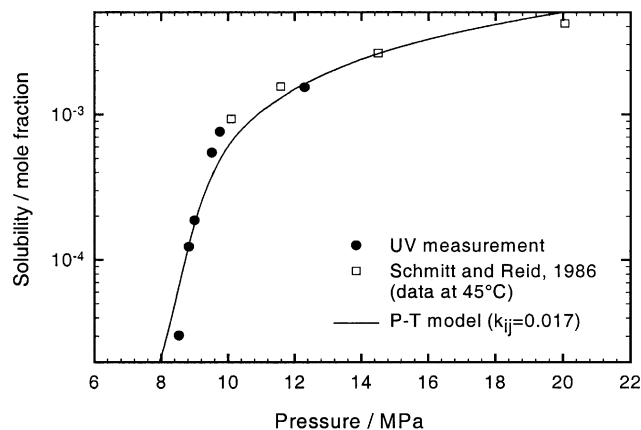


Figure 4. Solubility of 1,4-naphthoquinone in pure CO₂ at 313 K.

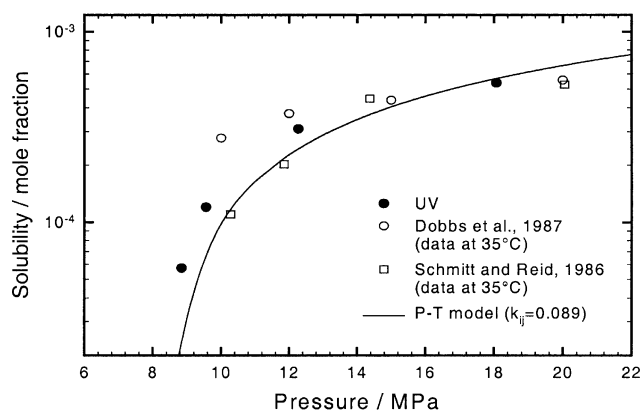


Figure 5. Solubility of 2-naphthol in pure CO₂ at 313 K.

For fluorescence measurements, the emission, E , follows the modified Beer's law, as below (Skoog and Leary, 1992):

$$E = KC,$$

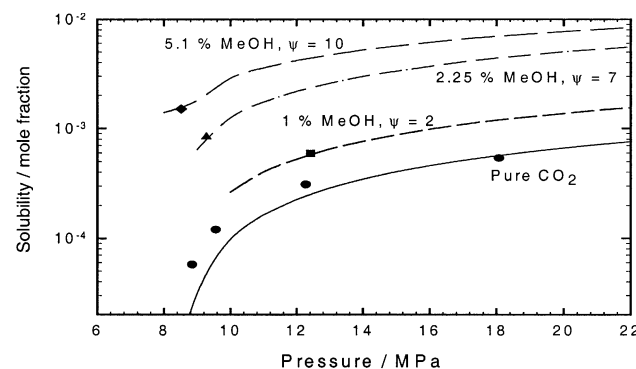


Figure 6. Patel-Teja fit for solubility of 1,4-naphthoquinone in pure CO₂ and methanol cosolvent at 313 K.

(—) Data fitting; (---) modeling; $\psi = \phi^0$ (binary)/ ϕ^0 (ternary).

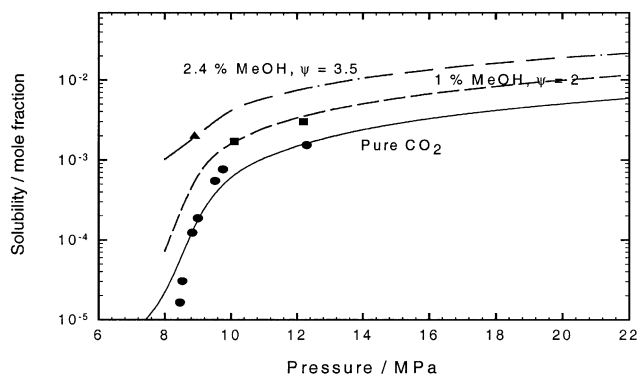


Figure 7. Patel-Teja fit for solubility of 2-naphthol in pure CO₂ and methanol cosolvent at 313 K.
(—) Data fitting; (---) Modeling; $\psi = \phi^0$ (binary)/ ϕ^0 (ternary).

where K is a constant that depends on ϵ , l , and other constants.

In our experiments, each solubility point was measured independently, and ϵ did not play a role in the calculation of solubility. No calibration or assumptions on ϵ were necessary, unlike the work of West et al. (1998), where extensive calibration for ϵ was required prior to solubility measurements. One trade-off for measuring solubility this way is the time necessary to obtain a solubility curve. However, in return, the data obtained using this method are very accurate and reliable. We were able to observe the diffusion of solute from the solid phase into the fluid phase. The time for the mixture to reach equilibrium typically varied from 1 h to 5 h, and was observed to take as long as 10 h when the solubility approached 10^{-2} mol fraction.

The results for anthracene in pure CO₂ show that the three spectroscopic techniques were consistent and that the data were reproducible. Experimental results show that IR is suitable for measuring the solubility of 10^{-5} or higher, UV is appropriate for solubility of 10^{-6} or higher, and fluorescence can measure solubility as low as 10^{-7} , all in mol fractions. Measurements done in IR and UV were found to be more convenient and easier to work with than fluorescence. In particular, UV was found to be the easiest technique due to the simplicity of the instrument and computer software. Furthermore, the fluorescence method is very sensitive and can be easily influenced by any side factors or any trace amounts of impurities present in the cell. Therefore, the cell had to be absolutely free of impurities prior to the experiments, and the windows had to be free of dust that could be accumulated from the air. Moreover, the cell chamber needed to be totally blocked from any source of lights from the environment.

Solubility data of anthracene were compared to data collected by Hampson (1996) and Kwiatkowski et al. (1984) at 313 K. Hampson (1996) obtained the solubility using a recirculating equilibrium procedure. Kwiatkowski et al. (1984) determined solubility using the flow technique. At higher pressures, our measured solubilities were consistently higher than data collected by Kwiatkowski et al. This could be due to the fact that in our method, equilibrium was allowed sufficient time, whereas in some other flow methods, the time was much

less. Moreover, other methods analyzed the composition of saturated solute/CO₂ mixture either by using a six-port valve and a sample loop (Hampson, 1996), or by relying on the mass differences in the equilibrium cell before and after CO₂ flow (Kwiatkowski et al., 1984). The errors associated with these methods for data analysis could become significant, especially at low solute concentrations, where CO₂ is highly compressible. Therefore, we believe that our solubility data are more accurate at lower pressures.

The solubilities of 1,4-naphthoquinone and 2-naphthol were measured by *in situ* UV spectroscopy only, due to the convenience of this method. However, we found that the solubility increases so much with cosolvent, and thus we only run the experiments with cosolvent at low pressures. Our results for 1,4-naphthoquinone are in good agreement with the data from Schmitt and Reid (1986). This is expected because the flow technique gives good reproducibility among different research groups in this solubility range. Our data for 2-naphthol do not compare well to the previous data from Dobbs and Johnston (1987) or to Schmitt and Reid (1986) (the two sources do not agree either). Again, we see disagreement when the solubility is below 10^{-3} .

To characterize these highly asymmetric mixtures, we need to use an equation of state that can represent the pure-component-phase behavior; otherwise, the binary interaction parameter will be correcting the pure component fugacity as well as the mixing rule. We chose the Patel-Teja equation of state (P-T), which contains four pure component parameters, T_c , P_c , F , and ζ_c . F and ζ_c are fit simultaneously to pure component vapor pressure and liquid molar volume data. Because anthracene, 2-naphthol, and 1,4-naphthoquinone exist as solids at the temperature of our measurements, we also included vapor pressure data for the hypothetical subcooled liquid in our fit of F and ζ_c , using the relationship

$$P_{\text{subcooled}} = P_{\text{sublimation}} \frac{\Delta H_{\text{fus}}}{R} \left(\frac{1}{T} - \frac{1}{T_{\text{fus}}} \right). \quad (1)$$

The best fit curves are also shown in Figures 3, 4 and 5. The interaction parameter is typical for CO₂-anthracene and CO₂-2-naphthol, but close to 0 for CO₂-1,4-naphthoquinone. We suggest that this may be due to Lewis-acid-Lewis-base-specific interactions between CO₂ and the carbonyl in 1,4-naphthoquinone, which would increase the solubility.

The prediction of the solubility of the two solids in CO₂ with methanol cosolvent from binary interaction parameters fit only from binary data was unsuccessful. Large cosolvent effects typically require a chemical-physical model (Ting et al., 1993), but can be modeled using an equation of state and one data point (Pouillot, 1995).

The solubility of a solid in a supercritical fluid is given by Eq. 2:

$$y_2 = \frac{P_2^{\text{sub}}}{P\phi_2} \exp \left(\frac{(P - P_2^{\text{sub}})v_2}{RT} \right) = \frac{P_2^{\text{sub}}}{P \exp \left[\frac{1}{RT} \int_0^P \left(\bar{v}_2 - \frac{RT}{P} \right) dP \right]} \times \exp \left(\frac{(P - P_2^{\text{sub}})v_2}{RT} \right). \quad (2)$$

We can use an equation of state to calculate the partial molar volume, but we have to integrate through the critical region where the equation of state is least accurate and the partial molar volume of the solute is large and negative. To bypass this problem, we break the integral in two parts,

$$\begin{aligned}\phi &= \exp \left[\frac{1}{RT} \left(\int_{P^0}^P \left(\bar{v}_2 - \frac{RT}{P} \right) dP + \int_{P^0}^P \left(\bar{v}_2 - \frac{RT}{P} \right) dP \right) \right] \\ &= \phi^0 \exp \left[\frac{1}{RT} \int_{P^0}^P \left(\bar{v}_2 - \frac{RT}{P} \right) dP \right], \quad (3)\end{aligned}$$

and use a solubility data point at P^0 to determine ϕ^0 .

Using Eqs. 2 and 3, the ratio of the solubility of a solid in a supercritical fluid with cosolvent (ternary) to that without cosolvent (binary) is given by

$$\begin{aligned}\frac{y_2(\text{ternary})}{y_2(\text{binary})} &= \frac{\phi^0(\text{binary})}{\phi^0(\text{ternary})} \exp \frac{1}{RT} \int_{P^0}^P [\bar{v}_2(\text{ternary}) \\ &\quad - \bar{v}_2(\text{binary})] dP. \quad (4)\end{aligned}$$

One ternary data point is used to calculate the ratio of the fugacity coefficients in the binary and ternary system at P^0 , and the P-T equation of state is used to evaluate the partial molar volumes at $P > P^0$. Extrapolations are shown in Figures 6 and 7 for constant compositions of cosolvent. Note that $\phi^0(\text{binary})/\phi^0(\text{ternary})$ changes with cosolvent composition and cannot be predicted from the P-T equation of state.

Conclusions

In conclusion, spectroscopy is a powerful tool for measuring the solubility of organic solids in supercritical fluids. Different spectroscopic techniques, including infrared, ultraviolet, and fluorescence, were utilized to measure the solubility of different organic solids in pure CO_2 and with cosolvent. No calibration is required, and as an additional benefit of this method, the molar absorptivity is determined at saturation. The solubility was observed to increase significantly with the presence of cosolvent due to intermolecular interactions between cosolvent molecules and solute or CO_2 molecules. A diagram summarizing the applicability of spectroscopy to solubility measurements is shown in Figure 8. In order to use spectroscopy to measure the solubility of an organic solid in scCO_2 , the chemical compound must show some absorption in the UV region, some IR absorption away from that of the solvent, or some fluorescence.

In summary, this spectroscopic method for measuring solubility has several advantages, as follows:

- It gives ways to measure solubility data over a wide range of concentrations, as low as 10^{-6} or 10^{-7} mol fraction.
- No calibration or assumption on ϵ is necessary. In fact, ϵ is determined at the solubility limit.
- The diffusion of solute from solid phase into fluid phase can be observed *in situ* to assure the equilibrium of solution mixture.

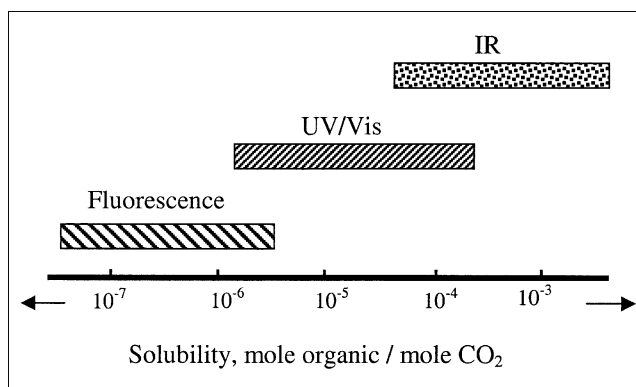


Figure 8. Different spectroscopic techniques for different solubility ranges.

However, this method also has a drawback in that it requires significant time to reach equilibrium.

Acknowledgment

The authors would like to thank the National Science Foundation (NSF) for its support; Dr. James Brown and Dr. Jie Lu for their suggestions on setting up the fluorescence experiments; and the two undergraduate students, Charles Tapley Gresham and Tram Dinh, for their assistance throughout the project.

Notation

A	= absorbance
C	= solute concentration, kmol/m ³
E	= fluorescence emission
F	= constant for Patel-Teja equation of state
K	= modified Beer's law constant
k_{ij}	= interaction parameter between component i and component j
l	= optical path length, m
P	= pressure, Pa or MPa
P_c	= critical pressure, Pa
P^0	= reference pressure, Pa
$P^{\text{sublimation}}, P^{\text{sub}}$	= sublimation pressure, Pa
$P^{\text{subcooled}}$	= vapor pressure of subcooled liquid, Pa
T	= temperature, K
T_c	= critical temperature, K
T_m	= melting temperature, K
R	= gas constant, J/mol·K
v_2	= molar volume of solute, m ³
y_2	= mol fraction of solute
ΔH_{fus}	= heat of fusion, J/mol

Greek letters

ϵ	= molar absorptivity, m ² /kmol
ϕ	= fugacity coefficient
ζ_c	= pure component constant for Patel-Teja equation of state

Subscripts

1	= CO_2
2	= solute
3	= cosolvent

Literature Cited

- Berger, T. A., "Density of Methanol-Carbon Dioxide Mixtures at Three Temperatures," *J. High Resolut. Chromatogr.*, **14**, 312 (1991).
- Colomina, M., M. V. Roux, and C. Turrión, "Thermochemical Properties of Naphthalene Compounds. II. Enthalpies of Combustion and Formation of the 1- and 2-Naphthols," *J. Chem. Therm.*, **6**, 571 (1974).
- Coutsikos, P., K. Magoulas, and D. Tassios, "Solubility of Phenols in Supercritical Carbon Dioxide," *J. Chem. Eng. Data*, **40**, 953 (1995).
- Cygnarowicz, L. L., R. J. Maxwell, and W. D. Seider, "Equilibrium Solubilities of β -Carotene in Supercritical Carbon Dioxide," *Fluid Phase Equilib.*, **59**, 57 (1990).
- De Kruif, C. G., E. J. Smit, and H. A. J. Govers, "Thermodynamic Properties of 1,4-Benzoquinone (BQ), 1,4-Hydroquinone (HQ), 1,4-Naphthoquinone (NHQ), and the Complexes BQ-HQ 1:1, NQ-HQ 1:1, NQ-NHQ 2:1, and NQ-NHQ 1:1," *J. Chem. Phys.*, **74**, 5838 (1981).
- Dobbs, J. M., and K. P. Johnston, "Selectivities in Pure and Mixed Supercritical Fluid Solvents," *Ind. Eng. Chem. Res.*, **26**, 1476 (1987).
- Ebeling, H., and E. U. Franck, "Spectroscopic Determination of Caffeine Solubility in Supercritical Carbon Dioxide," *Ber. Bunsenges. Phys. Chem.*, **88**, 862 (1984).
- Ely, J. F., W. M. Haynes, and B. C. Bain, "Isochoric (p,Vm,T) Measurements on CO₂ and on (0.982 CO₂ + 0.018 N₂) from 250 to 330 K at Pressures to 35 MPa," *J. Chem. Therm.*, **21**, 879 (1989).
- Hampson, J. W., "A Recirculation Equilibrium Procedure for Determining Organic Compound Solubility in Supercritical Fluids," *J. Chem. Eng. Data*, **41**, 97 (1996).
- Hansen, P. C., and C. A. Eckert, "An Improved Transpiration Method for the Measurement of Very Low Vapor Pressures," *J. Chem. Eng. Data*, **31**, 1 (1986).
- Inomata, H., Y. Yagi, M. Saito, and S. Saito, "Density Dependence of the Molar Absorption Coefficient—Application of the Beer-Lambert Law to Supercritical CO₂-Naphthalene Mixture," *J. Supercrit. Fluids*, **6**, 237 (1993).
- Jackson, K., L. E. Bowman, and J. L. Fulton, "Water Solubility Measurements in Supercritical Fluids and High-Pressure Liquids Using Near-Infrared Spectroscopy," *Anal. Chem.*, **67**, 2368 (1995).
- Johnston, K. P., D. H. Ziger, and C. A. Eckert, "Solubilities of Hydrocarbon Solids in Supercritical Fluids. The Augmented van der Waals Treatment," *Ind. Eng. Chem. Fundam.*, **21**, 191 (1982).
- Kazarian, S. G., M. F. Vincent, and C. A. Eckert, "Infrared Cell for Supercritical Fluid-Polymer Interactions," *Rev. Sci. Instrum.*, **67**, 1586 (1996).
- Kwiatkowski, J., Z. Lisicki, and W. Majewski, "An Experimental Method for Measuring Solubilities of Solids in Supercritical Fluids," *Ber. Bunsenges. Phys. Chem.*, **88**, 865 (1984).
- McHugh, M. A., and V. J. Krukons, *Supercritical Fluid Extraction: Principles and Practice*, Butterworth-Heinemann, Boston (1994).
- Miller, D. J., and S. B. Hawthorne, "Determination of Solubilities of Organics Solutes in Supercritical CO₂ by On-Line Flame Ionization Detection," *Anal. Chem.*, **67**, 273 (1995).
- Pouillot, F. L. L., *Thermodynamic and Spectroscopic Investigations of Solid-Supercritical Fluid Equilibrium*. PhD Diss., Georgia Institute of Technology, Atlanta (1995).
- Rice, J. K., E. D. Niemeyer, and F. V. Bright, "Evidence for Density-Dependent Changes in Solute Molar Absorptivities in Supercritical CO₂: Impact on Solubility Determination Practices," *Anal. Chem.*, **67**, 4354 (1995).
- Schmitt, W. J., and R. C. Reid, "Solubility of Monofunctional Organic Solids in Chemically Diverse Supercritical Fluids," *J. Chem. Eng. Data*, **31**, 204 (1986).
- Skoog, D. A., and J. J. Leary, *Principles of Instrumental Analysis*, Harcourt Brace, New York (1992).
- Ting, S. S. T., D. L. Tomasko, N. R. Foster, and S. J. Macnaughton, "Chemical-Physical Interpretation of Cosolvent Effects in Supercritical Fluids," *Ind. Eng. Chem. Res.*, **32**, 1482 (1993).
- West, B. L., S. G. Kazarian, M. F. Vincent, N. H. Brantley, and C. A. Eckert, "Supercritical Fluid Dyeing of PMMA Films with Azo-Dyes," *J. Appl. Polym. Sci.*, **69**, 911 (1998).
- Zerda, T. W., B. Wiegand, and J. Jonas, "FTIR Measurements of Solubilities of Anthracene in Supercritical CO₂," *J. Chem. Eng. Data*, **31**, 274 (1986).

Manuscript received Jan. 29, 2001, and revision received May 21, 2001.